SAND81-0114
Unlimited Release
UC-66
Printed February 1982

SAND--81-0114

DE82 009355

THE COOLING OF KILAUEA IKI LAVA LAKE

Richard G. Hills
Geothermal Research Division 4743
Sandia National Laboratories
Albuquerque, NM 87185

ABSTRACT

In 1959 Kilauea Iki erupted leaving a 110 to 120 m lake of molten lava in its crater. The resulting lava lake has provided a unique opportunity to study the cooling dynamics of a molten body and its associated hydrothermal system. Field measurements taken at Kilauea Iki indicate that the hydrothermal system above the cooling magma body goes through several stages, some of which are well modeled analytically. Field measurements also indicate that during most of the solidification period of the lake, cooling from above is controlled by 2-phase convection while conduction dominates the cooling of the lake from below. In this report, a summary of the field work related to the study of the cooling dynamics of Kilauea Iki is presented. Quantitative and qualitative cooling models for the lake are discussed.

MGW

DISCLAIMER

CONTENTS

LIST OF ILLUSTRATIONS

THE COOLING OF KILAUEA IKI LAVA LAKE

1.0 Introduction

The DOE-funded Sandia Magma Energy Research Project was initiated to study the scientific feasibility of extracting energy directly from buried magma sources. The project is divided into five main tasks; (1) Source Location and Definition, (2) Source Tapping, (3) Magma Characterization, (4) Material Compatibility, and (5) Energy Extraction.

As part of the Source Location and Definition task, the Magma Energy Research Project has been studying the shallow buried molten basalt body at Kilauea Iki lava lake. The lava lake was formed in 1959 when a series of eruptions from the southwest wall of Kilauea Iki left approximately 40×10^6 m^3 of new lava in the crater. After the 1959 eruption, the level of the lake stood 110 to 120 m above the original floor.

The Kilauea Iki lava lake provides a unique opportunity to study the cooling dynamics of a "live" magma body. This lake has been the subject of study by the United States Geological Survey (USGS) since 1959. With the creation of the Magma Energy Research Project in 1975, Sandia Laboratories (SL) has been studying the lake in conjunction with the USGS. The main emphasis of the joint USGS/Sandia effort has been to evaluate the effectiveness of various geophysical techniques in defining a "known" magma body. One of the techniques used to characterize the Kilauea Iki magma body is to measure temperatures in boreholes that are drilled directly into the magma body. The resulting temperature profiles also provide a cross-check on many of the surface geophysical techniques tested at

Kilauea Iki. In this report, a survey of the temperature measurements at Kilauea Iki is presented. Qualitative and quantitative models for the cooling of the lava lake are discussed.

2.0 Temperature Measurements

2.1 The Boreholes

Illustrated in Figure 2.1 are the locations of the boreholes used by the USGS and SNL to measure temperature profiles in the Kilauea Iki lava lake. As the figure indicates, most boreholes are located on a northerly radial from the center of the lake. A list of the boreholes used for temperature measurements at Kilauea Iki is presented in Table 2.1 along with the pertinent facts concerning the boreholes, such as geometry, dates of drilling and temperature measurements, and whether melt was encountered. As the table illustrates, over 90 temperature distributions have been measured in 21 holes.

2.2 The Temperature Probes

Most of the early temperature measurements (Richter and Moore, 1966) were made with 310 stainless-steel sheathed chromel-alumel thermocouples and a slide-wire potentiometer. Laboratory calibrations indicated an accuracy of 0.5% at 500°C and 1% at 1000°C for the thermocouple measurements. When conditions permitted, bottomhole temperatures were measured with incandescent filament-type optical pyrometers. For the shallow holes (holes 1 and 2), the pyrometers were found to be within a 5°C agreement of the temperatures obtained by the chromel-alumel thermocouples. In the deeper holes (the redrilled hole 2, and hole 3), a 10°C variation was was observed.

MAGMA ENERGY RESEARCH PROJECT

KILAUEA IKI LAVA LAKE LAKE DRILLHOLES

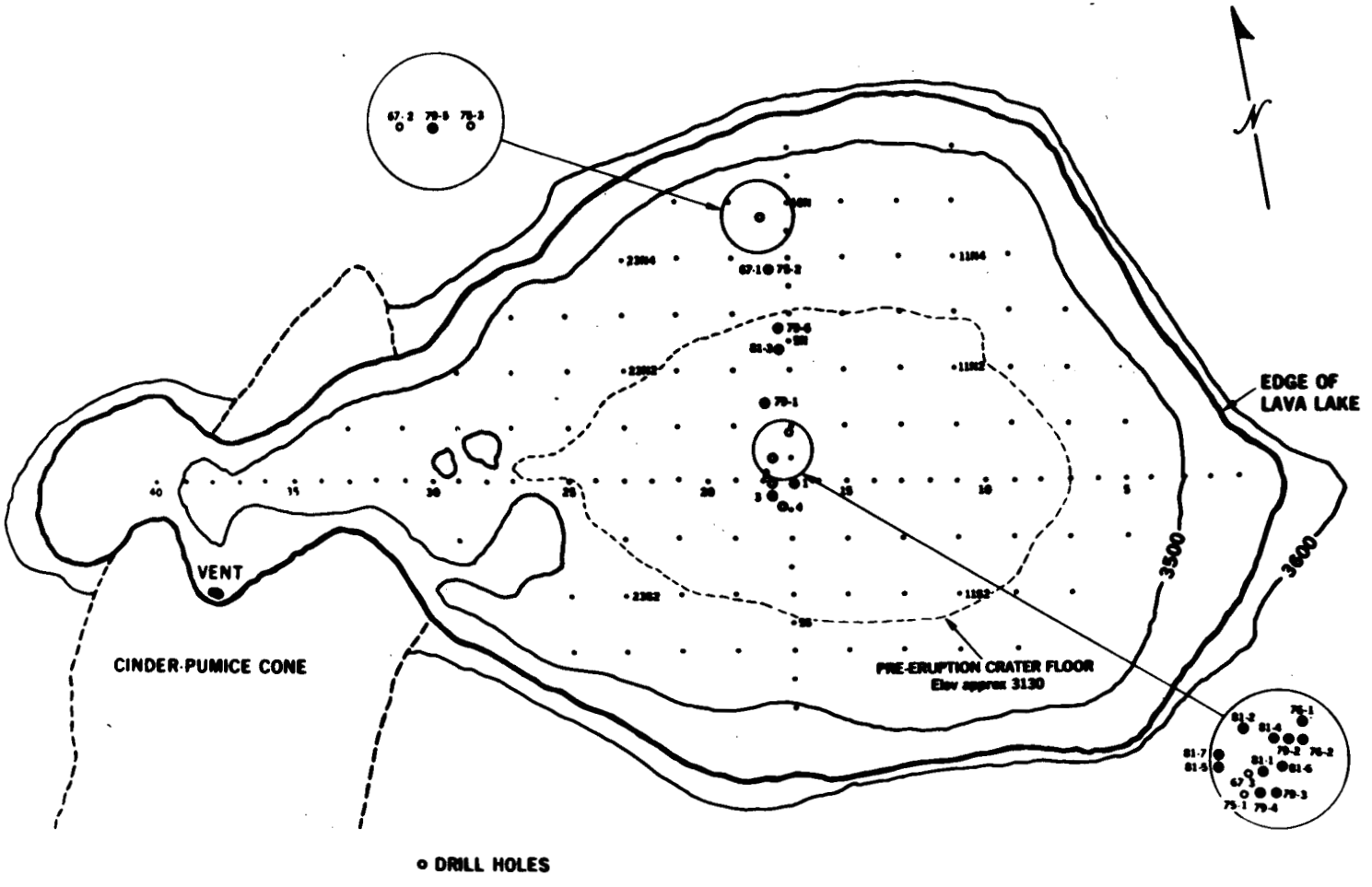

Figure 2.1 Kilauea Iki Lava Lake Borehole Locations

TABLE 2.1 Temperature Measurements

Hole No.	Drilling Agency	Date Drilled	Diameter, cm	Depth, m	Dates Measured	Greatest Depth Measured, m	Comments
1[1]	HVO	4-5/60	2.86	3.9	5/16/60	3.9	
	HVO	8/24/60	3.02	6.9	9/8/60	6.8	Hole 1 redrilled, melt encountered at 6.9 m during drilling
2[1]	HVO	4/13/61	3.02	9.3	10/2/61		Melt encountered at 9.1 m
	HVO	10/4/61	3.02	10.7	10/5/61	11.9	Hole redrilled, melt encountered at 10.7 m, stainless steel/ceramic probe forced 1.2 m into melt.
3[1]	HVO	5-6/62	3.02	12.8	6/21/62	12.6	Melt encountered at 12.7 m
4[1]	HVO	12/6/62	3.02	13.3			Melt encountered at 13.3 m
67-1[2]	HVO	3/67	7.6	25.9	3/8/67	24.3	Melt encountered at 25.9 m
					4/20/67	24.6	
					8/15/67	23.7	
					9/22/67	23.7	
					7/2/68	24.3	
67-2[2]	HVO	5-7/67	7.6	25.9	8/15/67	26.9	Melt encountered at 25.9 m
					9/22/67	26.3	
					7/5/68	25.9	
67-3 [2]	HVO	10/67	7.6	26.5	10/4/67	23.8	Melt encountered at 26.5 m
75-1[2]	HVO	2-3/75	7.6	44.0	6/5/75	40.2	Melt encountered at 44.2 m
					6/6/75	40.2	
					7/22/75	40.2	
					1/19/78	6.4	
					12/4/78	33.5	

TABLE 2.1 Temperature Measurements (cont'd)

Hole No.	Drilling Agency	Date Drilled	Diameter, cm	Depth, m	Dates Measured	Greatest Depth Measured, m	Comments
	SL/HVO			52.4	12/10/78	51.8	Hole redrilled to 52.4 m
					12/18/78		
					12/20/78	50.5	Hole cased with SS-316
					12/22/78	50.5	
					12/26/78	50.3	
					12/28/78	49.8	
					12/29/78	49.8	
					1/26/79	41.1	
					3/12/80	4.1	Hole blocked
					3/13/80	40.4	obstruction cleared
					4/5/80	40.3	
75-2[2]	HVO	2-3/75	7.6	42.5	3/27/75	39.2	Melt encountered at 42.5 m
					6/6/75	39.2	
					4/12/78	3.0	Hole blocked
75-3[2]	HVO	2-3/75	7.6	44.1	4/9/75	44.0	Melt encountered at 44.1 m
					6/10/75	35.8	
					4/12/78	17.9	Hole blocked
76-1[2]	SL/HVO	8/76	7/6	45.5	10/14/76	35.6	Melt encountered at 45.5 m
					11/19/76	41.9	
					12/20/76	41.8	
					4/12/78	39.8	
					12/4/78	39.6	
					12/5/78	39.6	
					12/6/78	39.6	
					12/7/78	39.6	
					12/8/78	39.6	
					12/9/78	6.1	
					1/6/79	38.9	
					3/17/79	41.3	
					3/12/80	37.5	
					[illegible]/80	37.6	

TABLE 2.1 Temperature Measurements (cont'd)

Hole No.	Drilling Agency	Date Drilled	Diameter, cm	Depth, m	Dates Measured	Greatest Depth Measured, m	Comments
76-2[2]	SL/HVO	8-9/76	7.6	45.7	10/14/76	41.5	Melt encountered at 45.7 m
					11/19/76	41.4	
					12/20/76	41.5	
					3/17/79	38.1	
					4/5/80	24.3	
79-1[3]	SL/HVO	12/79	9.6	61.7	12/22/78	61.4	Melt encountered at 50 m[4]
					12/24/78	48.8	
					12/29/78	51.8	
					12/31/78	51.6	
					1/6/79	50.7	
					1/24/79	48.8	
					2/12/79	50.0	
					2/13/79	54.3	
					7/24/79	52.4	
					7/26/79	52.5	
					3/11/80	43.3	
					4/5/80	48.9	
79-2[3]	SL/HVO	12/79 - 1/80	9.6	50.5	3/16/79	48.7	Hole collapsed night after drilling
					3/13/80	39.1	
					4/5/80	2.6	Hole obstructed at 2.6 m
79-3[3]	SL/HVO	1/79	9.6	51.8	1/26/79	45.4	Melt encountered at 52.6 m, melt flowed uphole leaving 51.8 m open
					2/13/79	48.5	
					2/14/79	48.5	
					3/16/79	48.7	
					5/23/79	48.8	
					7/24/79	48.5	
					3/13/80	39.1	
					4/5/80	8.7	Hole obstructed

TABLE 2.1 Temperature Measurements (cont'd)

Hole No.	Drilling Agency	Date Drilled	Diameter, cm	Depth, m	Dates Measured	Greatest Depth Measured, m	Comments
79-4[3]	SL/HVO	1/79	9.6	51.2	1/26/79	34.7	Melt encountered at 54.8 m, melt flowed uphole leaving 51.2 m open, Hole cased with SS-316 in lower 12.2 m and carbon steel casing to surface.
					3/12/80	38.5	
79-5[3]	SL/HVO	2/79	9.6	104.2	2/8/79	92.7	Hole on margin of molten lens, did not encounter melt.
					2/15/79	99.7	
					2/17/79	99.7	
					3/16/79	98.5	
					4/26/79	98.1	
					5/23/79	98.5	
					7/24/79	98.0	
					7/26/79	98.0	
					3/10/80	97.3	
					4/4/80	97.5	
					4/6/81	97.1	
79-6[3]	SL/HVO	2/79	9.6	58.5	3/16/79	42.9	Melt encountered at 58.5 m, melt flowed uphole leaving 45.7 m open
					3/11/80	42.8	
81-1[4]	SL/HVO	4/81	6.0	93.6	4/29/81	37.2	Obstruction encountered in 3/4" SS-310 casing.
					5/1/81	58.8	Used smaller dia. probe, obstruction encountered.
81-2[4]	SL/HVO	4/81	7.6	71.9	5/1/81	61.5	Cased down to 67.1 m with BW casing, obstruction encountered at 61.5 m.
81-3[4]	SL/HVO	4/81	6.0		4/29/81	46.5	Obstruction encountered in 3/4" SS-310 casing

[1] Richter and Moore, 1966
[2] Colp and Okamura, 1978
[3] Colp, 1980
[4] Dunn, 1981

As experience was gained, changes were made in the temperature measuring apparatus that lead to quicker measurements with less chance for human error. For example, later measurements were made with either a Comark electronic thermometer with a sweep needle indicator or a Doric Trendicator with a digital readout. Both of these instruments indicate temperature directly.

Further improvements to the thermocouple probe were made by Colp and Striker (Colp and Striker, 1980) during the winter of 1978. Originally, distance below the surface was indicated by strips of equally spaced metallic tape attached directly to the thermocouple sheathing. Unfortunately, the high temperature encountered in the boreholes led to failure of the tape's adhesive. In the most recent experiments, the depth of measurement was determined by an Olympic wire length meter. The meter consists of a roller assembly through which the sheathed thermocouple is passed. A digital indicator on the assembly reads out the length of the wire passed through the roller assembly to the nearest 3 cm (1 inch). Laboratory experiments indicate that the error in measuring a stainless steel sheathed thermocouple lead at a uniform temperature is less than 5 cm over 100 m. Errors introduced due to thermal expansion of the lead at the elevated temperatures led to much more serious errors. For example, in a hole 100 m deep with an average temperature of 500°C, the error will be approximately 60 cm. Although a theoretical correction for thermal expansion is possible, no corrections have been applied to the measurements discussed here.

A second design refinement (Colp and Striker, 1980) was the development of a stainless steel probe assembly (see Figure 2.2), which weighs approximately 1 kg, and is designed to protect the thermocouple tip with a minimum of thermal mass. The previous probe consisted of a thermal couple surrounded by a perforated pipe. Field measurements at Kilauea Iki indicate that the latest probe stabilizes to within the noise level of the measurement ($\pm$ 1°C) within 1 minute when the probe was allowed to equilibrate every 3 m.

In addition to cable length and temperature measurement errors, discrepancies between measured temperature and true formation temperature exist

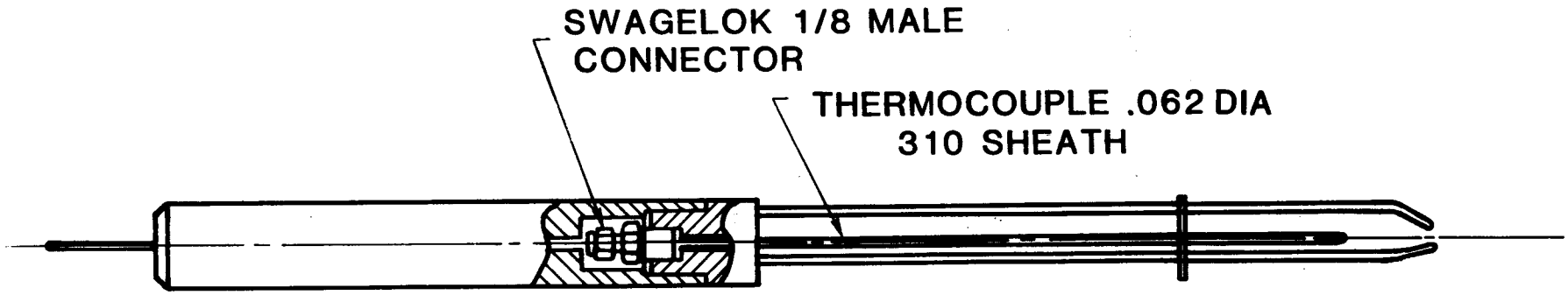

FIGURE 2.2 TEMPERATURE PROBE

due to the effects of steam flowing uphole. Since these errors involve the cooling dynamics of the formation and not instrument error, they will be discussed in the following sections.

3.0 Cooling Models for Kilauea Iki Lava Lake

As the contents of Table 2.1 illustrate, over 90 borehole temperature profiles have been recorded for Kilauea Iki lava lake. In this report, only those profiles that contribute significantly to the interpretation of cooling models will be presented. The following discussion is divided into several sections. The first section reviews thermal crack propagation which significantly affects hydrothermal circulation. The next sections discuss the cooling dynamics of the region over the center of the molten body, in the margins, and in the region below the molten body respectively. As the discussion will show, knowledge of the cooling dynamics of the Kilauea Iki lava lake is the highest for the region over the center of the body, and the lowest for the margins of the body.

3.1 Thermal Fracturing

Laboratory experiments by Dunn (Colp 1979) determined that the permeability of a 6.35 cm dia., 11.4 cm long competent core sample taken from the Kilauea Iki 76-2 hole at a depth of 37.8 m was 0.005 Darcy. In-situ experiments by Dunn (Colp, 1979) show that the effective permeability of Kilauea Iki basalt can range from 0.092 Darcy to 0.3 Darcy. Inspection of the complete set of core samples indicates that the higher field permeability was due to fractures in the rock. The importance of the fractures on hydrothermal convection cannot be overemphasized.

Ryan (1979) has studied the propagation of thermally induced fractures in Hawaiian type basalt. Ryan's scenario for thermal crack propagation is as follows: As the molten basalt solidifies and cools to some critical temperature, elastic stresses build up. At a critical temperature, which depends on the modal mineralogy, cooling rate, and volume fraction of glass, a crack forms which propagates toward the high temperature zone. The propagation halts when it reaches a temperature where viscous flow can occur in the intercrystalline glass. This cycle repeats as the body cools. For example, Ryan suggests that for the basalt of the Boiling Pots of Hawaii, the upper and lower temperature are approximately 725°C and 675°C.

The existence of thermally induced cracks can increase the hydrothermal cooling rate of magma bodies. As discussed in the following sections, the cracks can have differing effects on the rate of cooling depending on their location relative to the magma body.

3.2 Heat Transfer Over the Center of the Molten Body

Since the 1959 eruption, the Kilauea Iki lava lake has been solidifying at a rate that depends on the thermal mechanisms present during the various stages of cooling. A review of the cooling history over the center of the molten body during its early stages of cooling is given by Hardee (1980) who also presents a quantitative model for one of these stages.

The rate of movement of the upper solidification front during the early cooling is illustrated in Figure 3.1. Hardee used the 1070° C isotherm to define the location of the solidification front. In previous

work (Peck, 1978; Richter and Moore, 1966), the 1070°C isotherm was somewhat arbitrarily chosen to mark the solidification boundary (no discrete boundary actually exists) since this value represented the softening temperature of lava under the conditions encountered at several lava lakes in Hawaii. As a matter of consistency, the 1070°C isotherm is also used here to arbitrarily mark the solidification front. Shown in the figure are two square-root-of-time curves, and the curve derived by Hardee. The classical square-root-of-time curve of Carslaw and Jaeger (1959) is based on a one-dimensional pure conduction model, (see Hardee, 1980, for the estimates of the thermal properties) whereas the curve of Peck, Moore, and Kojima (1964) is based on a curve fit of observations taken during the post-1963 solidification of the Alae lava lake in Hawaii. The measured depths are indicated by the solid squares. Due to the greater depth of the Kilauea Iki lava lake (120 m vs. 15 m), Kilauea Iki has a more complicated cooling history than Alae. During the initial solidification of Kilaueau Iki, the square-root-of-time curve of Peck et al. (1964) was well matched (see Figure 3.1). The agreement between Peck's curve and the observations at Kilauea Iki suggest that the meteoric conditions and the thermal properties of the two lakes were similar. One cannot expect Peck's curve to be appropriate at a location where vastly different conditions exist. However, since the square-root-of-time behavior is characteristic of a purely conducting media, and such a behavior seems to model Alae during most of its solidification stage, and to model Kilauea Iki during its first stage of cooling, the first stage of cooling of a lava lake in a less wet location can probably by well represented be the square-root-of-time curve where the thermal conductivity is taken as an effective valve to account for the cooling

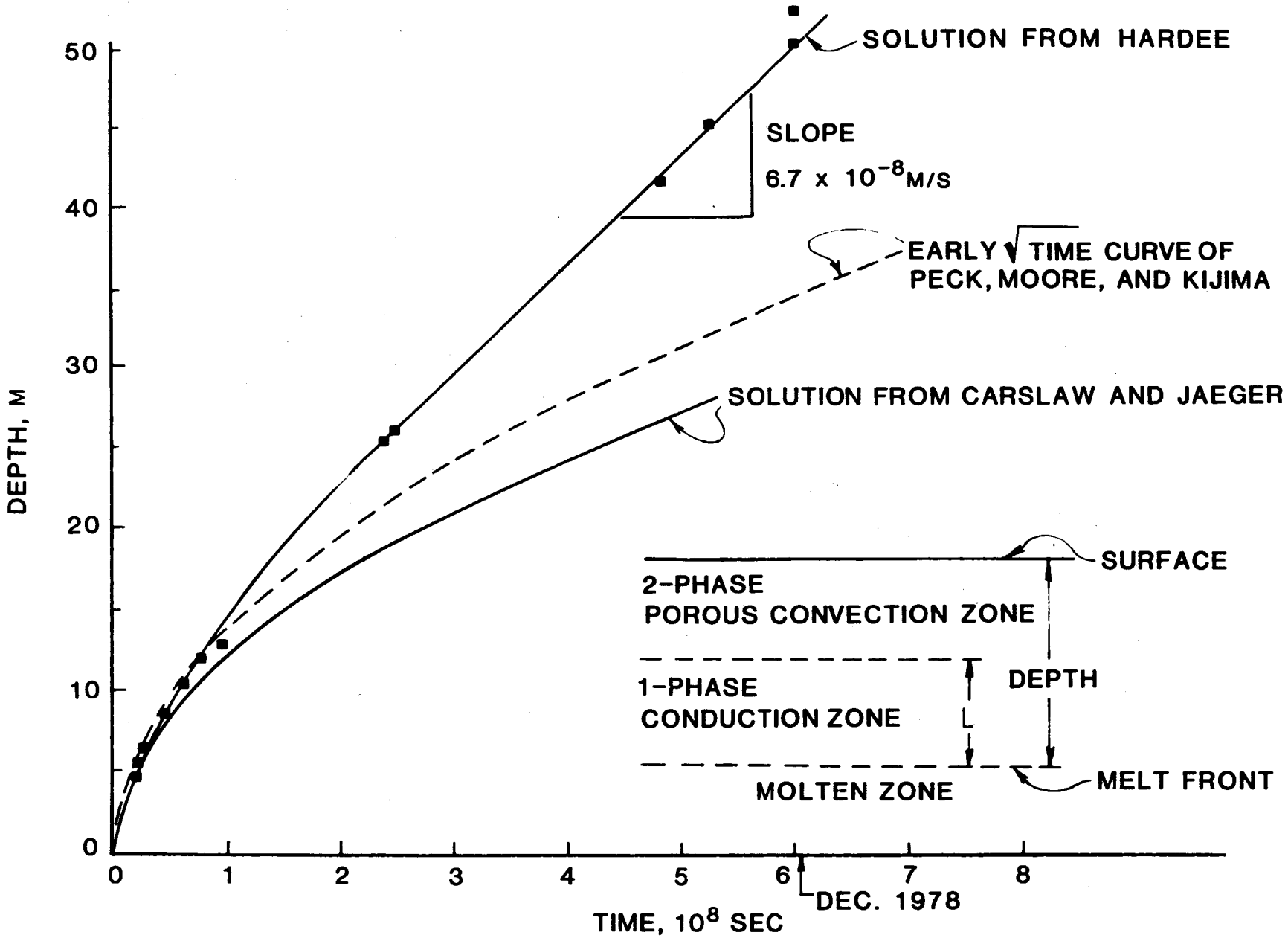

FIGURE 3.1 DEPTH TO SOLIDIFICATION FRONT

effect of rain.

During the second stage of cooling (after 6 years), the solidification front moves downward at a constant velocity of 6.7×10^{-8} m/s (2.1 m/year) rather than with the square-root-of-time. Hardee (1980) suggests that the constant rate of solidification during this stage is due to the controlling nature of a 2-phase convection zone of the meteoric water above the partial melt. Hardee's model for the second stage of cooling is illustrated in Figure 3.2. During this stage, the high temperature zone above the solidification front is at a sufficient depth to allow liquid water and steam to coexist in the formation above. In this zone, heat transfer is controlled by 2-phase convection. The maximum heat transferred due to the convection is, in turn, controlled by the effective permeability of the formation. Since the effective permeability is essentially constant over the length scales involved ($\sim$10 m), the heat transferred and thus the rate of solidification of the magma is essentially constant. Between the 2-phase zone and the magma is a conduction-dominated transition zone in which the temperature increases from boiling (100°C) to that of the melt (1070°C). Superheated steam exists in this zone, but does not convect since the Rayleigh number in this zone is 4 orders of magnitude less than the critical Rayleigh number (Hardee, 1980). Agreement between Hardee's model for the resulting time-dependent temperature distribution above the magma body and observation is excellent. However, as the lake solidifies to a point where the lower and upper solidification fronts are in close proximity, the solidification rate is expected to change. This change represents the third stage of solidification.

Presently, there is no direct evidence supporting the idea that the central region of the lake has entered the third stage of solidification.

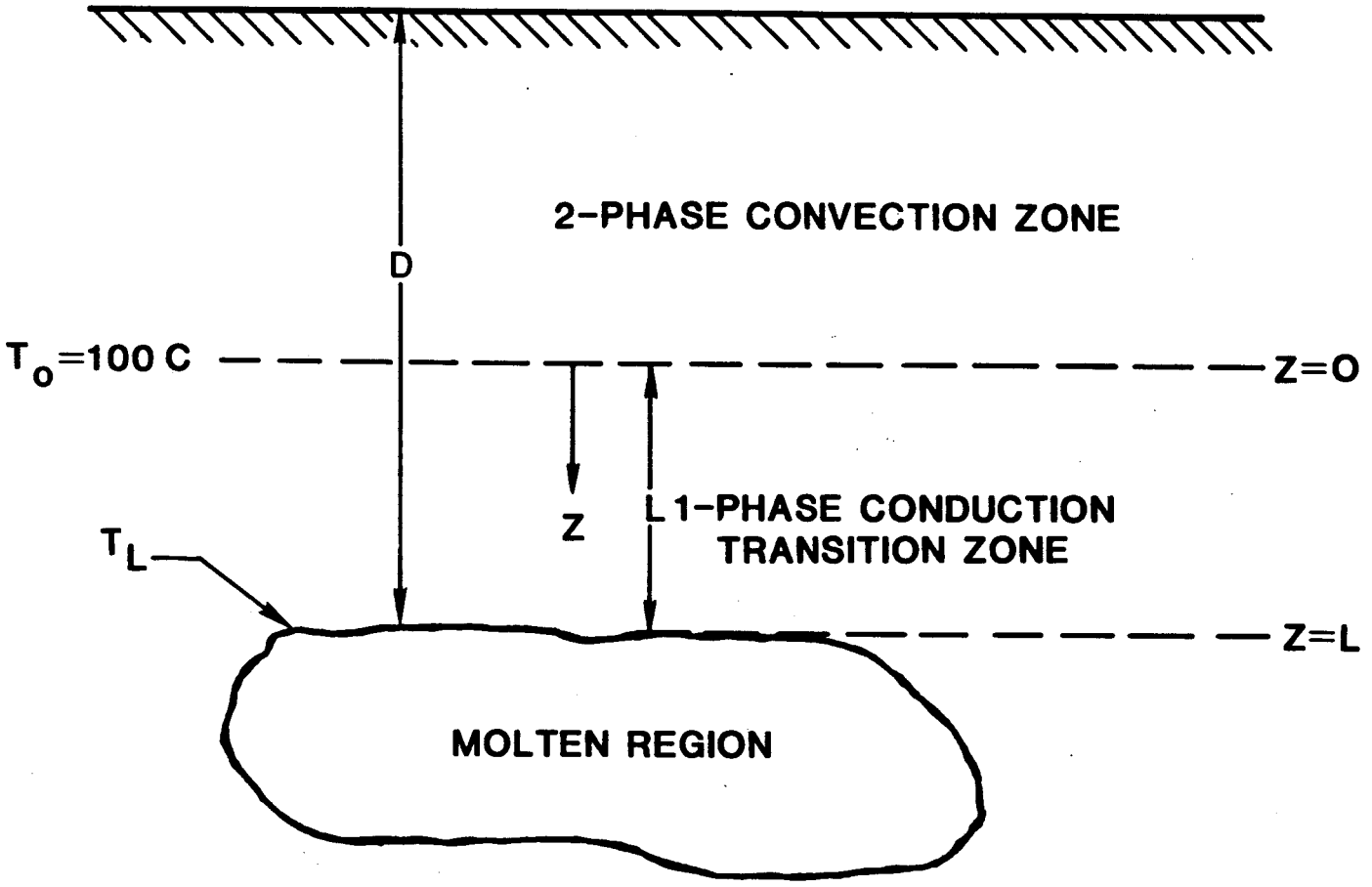

FIGURE 3.2 THERMAL MODEL FOR KILAUEA IKI LAVA LAKE

However, recent measurements [Hardee, (1980)] do suggest that a third stage of cooling has been entered in a region near the edge of the molten lens. Hardee suggests that the onset of this stage of cooling is reflected by a change in the characteristic curvature of the temperature versus depth profile above the partial melt. Such a change has been observed in hole 79-1 (see Figure 2.1). The onset of the third stage of cooling represents the point in time at which the maximum melt temperature departs significantly from the temperature at which the lake originally formed due to the close proximity of the upper and lower solidification fronts. Although direct depth measurements showing the acceleration of the solidification front do not exist for Kilauea Iki at the present time, Peck (1978) has reported an increased solidification rate for Alae lava lake, Hawaii, during its later stages of solidification. When the upper and lower solidification fronts coincide and the lake is solidified, the fourth stage of cooling begins.

If Ryan's (1979) thermally induced fracturing model is correct, and applicable to Kilauea Iki basalt, the fourth stage of cooling can be defined by that stage after which solidification is complete, but before thermal fracturing has taken place in the high temperature region of the lake. Heat transfer in the high temperature region (725°C, see Ryan, 1979) will be conduction dominated.

Once the temperature decreases to a point where thermal fractures exist throughout the formation, hydrothermal circulation of superheated steam could exist throughout the high temperature region of the lake. The rate of the cooling during this stage (stage 5) will depend to a certain extent on the availability of water from below. Hydrothermal

circulation induced by hot spots in saturated porous media has been studied analytically by many authors (Cheng and Minkowycz, 1977; Hardee, 1976; Hickox, 1977; Norton and Knight, 1977; Parmentier, 1979; Schubert and Strauss, 1979; Strauss and Schubert, 1977). If the high temperature region of the lake is surrounded by a water-saturated formation, then a convective system will probably exist with upwelling superheated steam passing through the high temperature region near the center of the lake, and with liquid water descending through the low temperature region on the margins of the lake.

As the lake continues to cool, the lake will enter the last stage of cooling (stage 6) in which all the water is at a temperature below its boiling point. In this stage the lake will continue to cool by conduction and downward percolation of water to ambient conditions.

While the first 2 stages of cooling have been verified by field measurements at Kilauea Iki, the last 4 stages of cooling have not. Until field verification is possible, the suggested mechanisms of heat transfer for Kilauea Iki during the later stages can only be speculative.

3.3 Heat Transfer Beneath the Magma Body

The only location at which temperature measurements have been made down to the pre-1959 surface is in 79-5 (see Figure 2.1). This hole is on the margin of the lake and does not penetrate the partial melt zone at the lake's center. No holes exist in which temperatures can be measured directly beneath the melt.

Analysis of core samples by Luth, Gerlach, and Eichelberger

(1981) from the 1981 drilling at Kilauea Iki suggests that the zone above 1070°C, at the time of drilling, extended from 60.5 to 89.5 m below the surface. Since the depth to the pre-1959 surface is between 110 m and 120 m, the lower 1070°C isotherm would have had to move upward at an average rate of 0.9 to 1.4 m/year. A pure conduction rate of solidification can be estimated from the results obtained by Carslaw and and Jaeger (1959). They find that a lower solidification front at T_1 would have the following displacement with time:

$$X = 2\lambda\sqrt{\alpha t} \tag{3.1}$$

where λ is defined by

$$\lambda e^{\lambda^2}[1 + \mathrm{erf}\lambda] = \frac{C_m T_1}{\mathcal{L}\sqrt{\pi}} \tag{3.2}$$

and

C_m - specific heat of lava, 1046 J/kg

$\mathcal{L}$ - latent heat of solidification, 4.18×10^5 J/kg

T_1 - solidification temperature above ambient, choose 1050°C = 1070°C - 20°C

t - time, s

X - distance to solidification front from its initial position

α - thermal diffusivity, 5×10^{-7} m^2/s

λ - characteristic value, 0.622 for properties given above

After 22 years (6.9×10^8 s), Eq. (3.1) gives the displacement of the lower solidification front to be 23 m, which corresponds to an average solidification rate of 1.1 m/year. This value is consistent with observation suggesting that a pure conduction model for the region below the lower 1070°C isotherm is adequate.

3.4 Heat Transfer on the Lateral Margins of the Magma Body

A cross-section depicting several of the boreholes drilled in 1979 is shown in Figure 3.3. The deepest borehole drilled to date is 79-5, which is on the margin of the molten body. A plot of the temperature distribution at various times since the drilling of the hole is shown in Figure 3.4. The figure illustrates that the temperature within the hole has been increasing throughout its depth since drilling. The first few months of heating represent the return to quasi-equilibrium from the artificially cooled condition caused by the drilling water.

The behavior in the 70-100 m depth range of 79-5 suggests that some type of transient heat source is present at depth. A possibility for the transient source is that the continuing cooling of the lava lake caused new thermal fractures that resulted in a new circulation pattern extending laterally from the high temperature region to a location near 79-5. At present, there has been no analytical or experimental verification of this hypothesis.

A second unexpected trend in the temperature profile of 79-5 is illustrated in Figure 3.5. In the figure, temperature as a function of depth for the upper 50 m of 79-5 is plotted. The temperatures labeled "INITIAL CONDITION" are the temperatures measured by Graeber on 4/26/79 (see Figure 3.4). The measurements observed 11 months later were taken by Colp and Hills on 3/10/80. The expected change in temperature over the same 11-month period due to one-dimensional conduction (thermal diffusivity = 5×10^{-7} m^2/s) is also shown. The discrepancy between

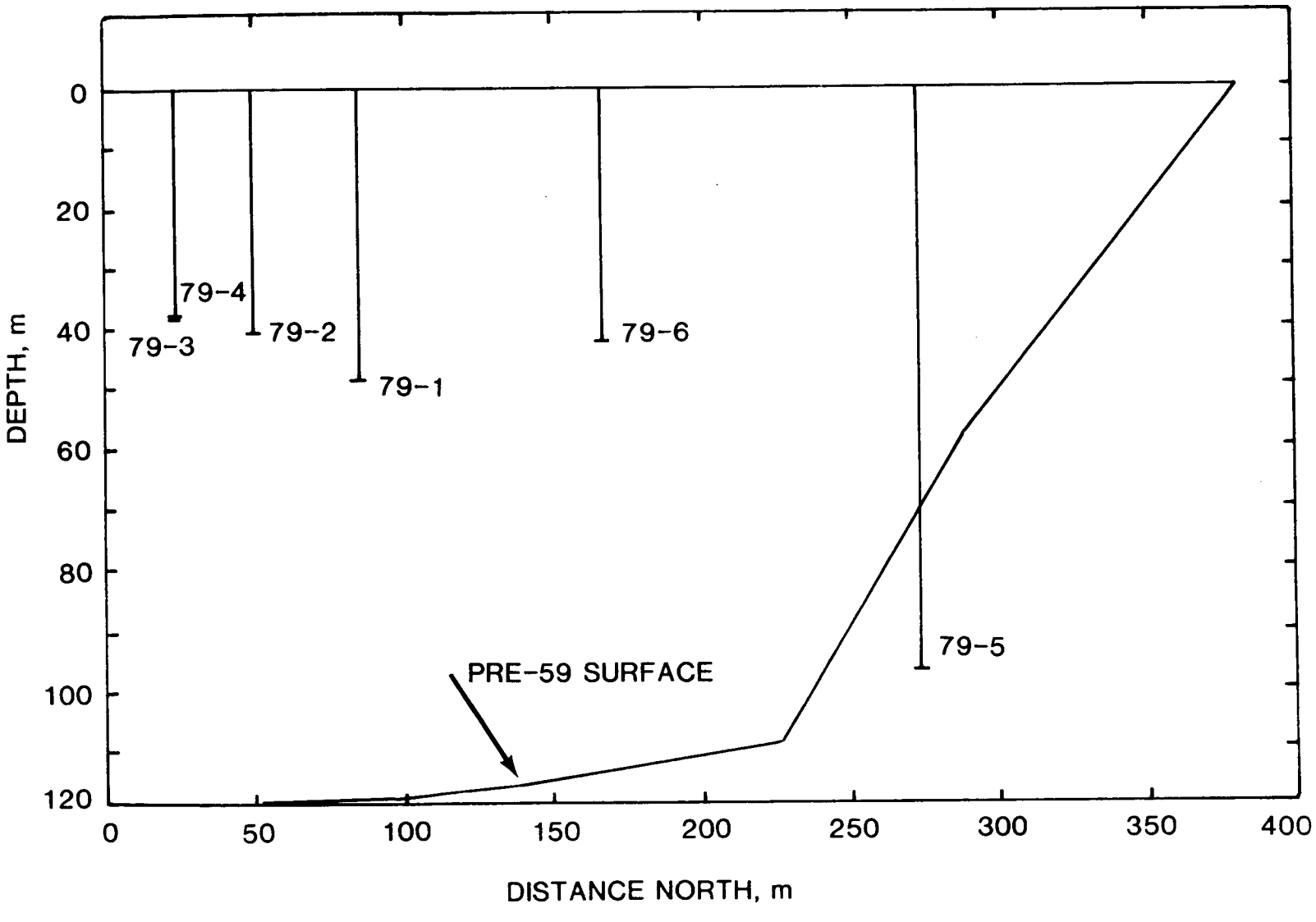

FIGURE 3.3 CROSS-SECTION OF KILAUEA IKI LAVA LAKE

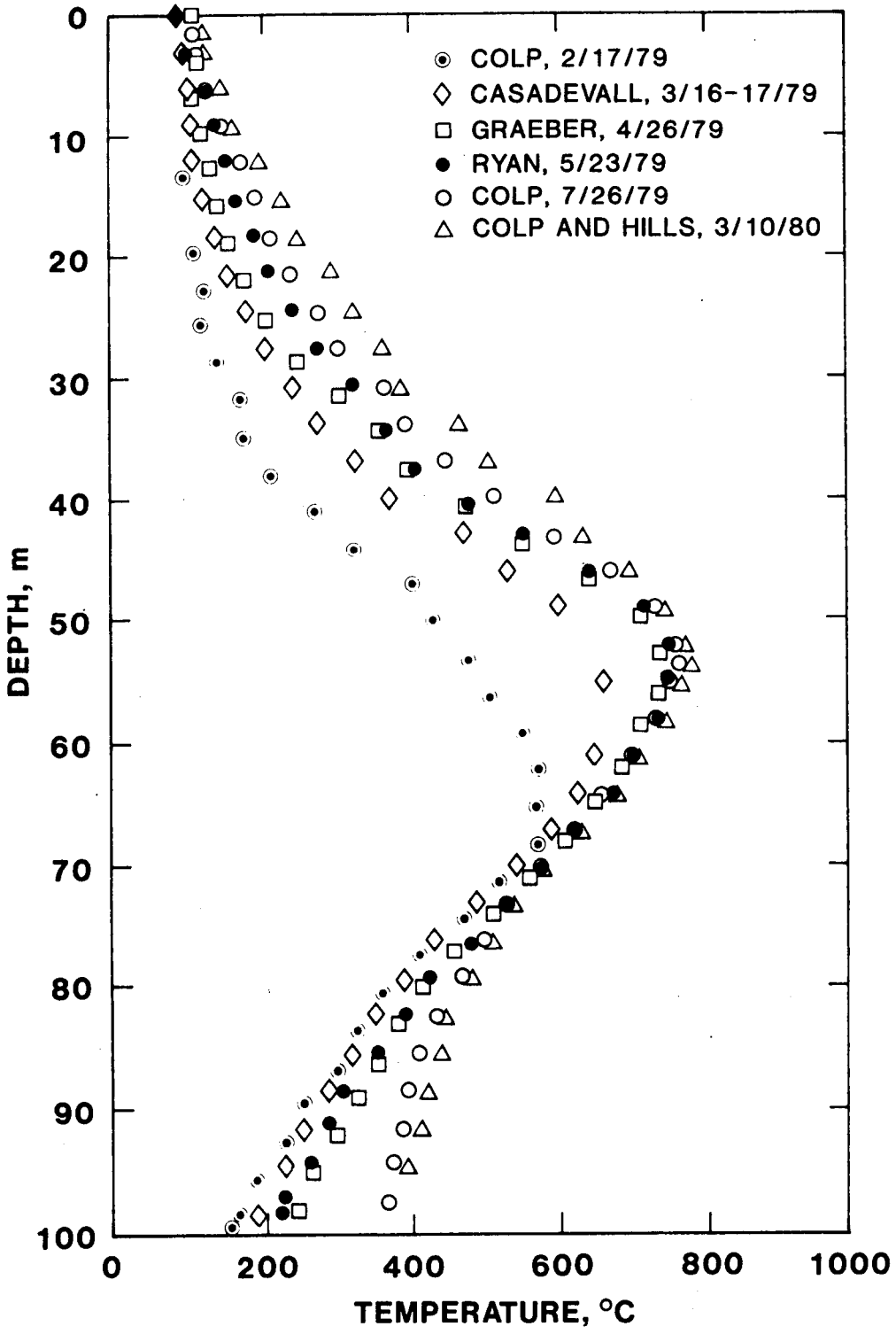

FIGURE 3.4 TEMPERATURE PROFILES IN 79-5

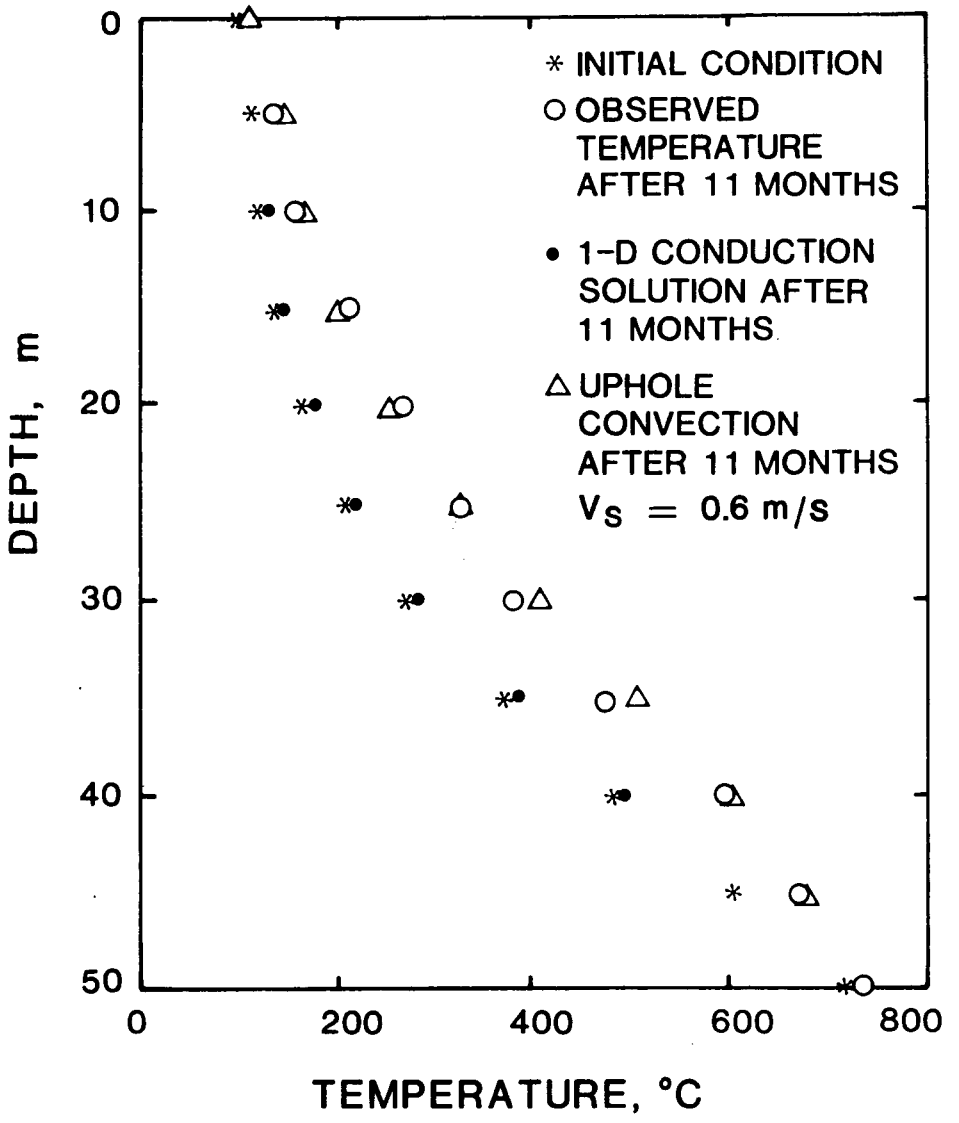

FIGURE 3.5 EFFECT OF STEAM FLOW IN A BOREHOLE

observation and one-dimensional conduction theory is as much as 100°C. A second discrepancy in the behavior of the upper 50 m of 79-5 is the fact that temperatures above 100°C are observed within 5 m of the surface during March of 1980, whereas over the hotter center region of the lake, the super 100°C region is not observable within 30 m of the surface in 79-3, or observable at all in the other holes ($\sim$40 m depth).

A probable reason for the unexpected behavior in the upper 50 m of 79-5 is the effect that the upflowing steam has on the long-term temperature measurements. Steam flowing uphole from the high temperature region below will not only affect the thermocouple measurements, but will also slowly heat the borehole walls.

To study the temperature influence of the steam flowing uphole, a numerical model was developed. The coordinate system used for the model is illustrated in Figure 3.6. An energy balance for pure conduction in the formation surrounding the borehole was modeled by

$$\rho c_p \frac{\partial T}{\partial t} = k\left[\frac{1}{r}\frac{\partial}{\partial r}\left(r\frac{\partial T}{\partial r}\right) + \frac{\partial^2 T}{\partial z^2}\right] \tag{3.3}$$

with the conditions on T(r,z,t);

$$T(r,z,0) = T_i(z) \tag{3.4a}$$

$$h(T(a,z,t) - T_s(z,t)) = k\frac{\partial T}{\partial r}(a,z,t) \tag{3.4b}$$

$$\lim_{r\to\infty} \frac{\partial T}{\partial r}(r,z,t) = 0 \tag{3.4c}$$

$$T(r,0,t) = T_o \tag{3.4d}$$

$$T(r,d,t) = T_d \tag{3.4e}$$

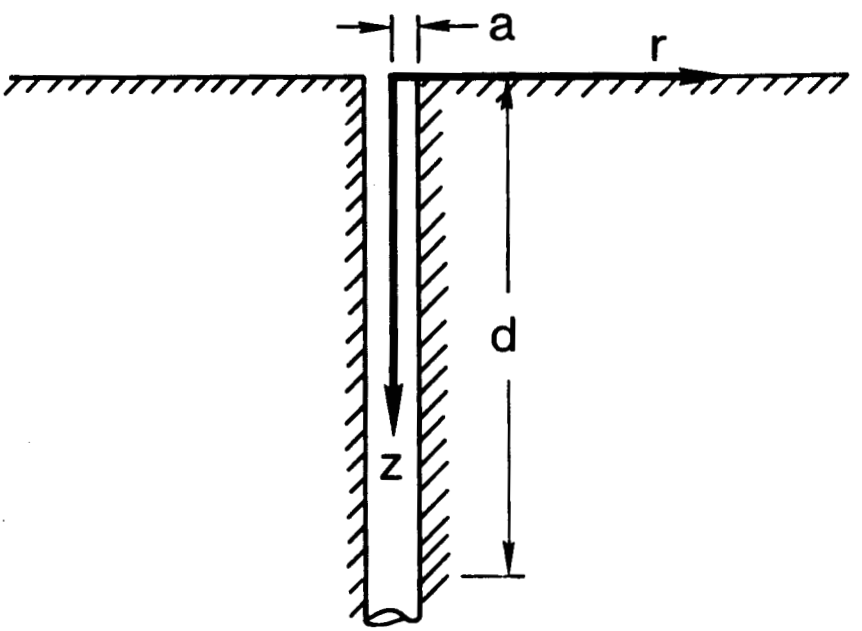

FIGURE 3.6 COORDINATE SYSTEM

V_s - speed of steam flowing uphole

α_s - thermal diffusivity of steam, 1.08×10^{-4} m^2/s

ν_s - kinematic viscosity of steam, 8.19×10^{-5} m^2/s

The energy balance of the steam flowing in the open borehole was taken to be

$$\rho_s C_{p_s} \overline{V}_s \frac{\partial T_s}{\partial z} = \frac{2k}{a} \frac{\partial T}{\partial r}\bigg|_a \tag{3.9}$$

with the conditions on $T_s(z,t)$;

$$T_s(z,o) = T_i(z) \tag{3.10a}$$

$$T_s(d,t) = T_d \tag{3.10b}$$

where

C_{p_s} - specific heat of the steam, 2008 J/kg°C

$\overline{V}_s$ - velocity of the steam, m/s

ρ_s - density of the steam, 0.303 kg/m^3

Note that the temperature dependence of the thermal properties of the steam and the formation are neglected. The precision gained by introducing temperature dependent properties is not warranted here. The energy balance given by Eqs. (3.9) and (3.10) states that the increase in temperature of the flowing steam is due to energy conducted into the steam from the formation. The transient response of the steam is neglected (i.e. $\partial T_s/\partial t \sim 0$) since the thermal response time of the steam is very quick relative to that of the formation.

An explicit finite difference approximation was used to model Eq. (3.3). The second boundary condition on the formation energy balance,

Eq. (3.4b), was modeled by using an imaginary node and a central difference for the derivative to give second order accuracy.

An explicit equation for T_s in terms of the borehole wall temperature can be derived from Eq. (3.9). The substitution of Eq. (3.4b) into Eq. (3.9) gives

$$\frac{\partial T_s}{\partial z} + \beta T_s = \beta T(a,z,t) \tag{3.11}$$

where

$$\beta = \frac{2h}{a\rho_s C_{p_s} \sqrt{V_s}} \quad . \tag{3.12}$$

Integration of Eq. (3.11) gives

$$T_s(z,t) = \beta e^{-\beta z} \int_o^z T(a,\lambda,t) e^{\beta\lambda} \, d_\lambda + Ce^{-\beta z} \tag{3.13}$$

Note that the velocity was assumed to be constant. Applying the boundary condition on T_s, Eq. (3.10b), gives

$$T_s(z,t) = \beta e^{-\beta z} \int_d^z T(a,\lambda,t) e^{\beta\lambda} \, d_\lambda + T_d e^{\beta(d-z)} \tag{3.14}$$

Since the finite difference approximation will give T(a,z,t) only at discrete points along z, an integration technique that uses only the values of T at these points was used to evaluate Eq. (3.14) A trapezoidal technique was felt to be adequate.

The results of using the temperature measurements in 79-5 on 2/17/79 as an initial condition, $T_i(z)$, and holding the upper and lower boundaries (z = 0,d) at 100°C and 720°C for a steam velocity of $\overline{V}_s$ = - 0.6 m/s (0.6 m/s uphole flow) are illustrated in Figure 3.5. The "Δ" gives the models' predictions for steam temperature at various depths (the downhole thermocouple measures steam temperature which is, in general, different from

borehole wall temperature) in the borehole after 11 months of steam contamination. As the figure illustrates, agreement between prediction and observation is good. The second order differences are probably due to the simplistic nature of some of the approximations used in the model. The radial temperature distribution obtained at two depths by the model after 11 months of steam heating is illustrated in Figure 3.7. Note the rapid drop-off in temperature as one moves into the formation at 30 m depth. Differences between borehole wall temperature (r = a) and the formation temperature are as much as 100°C. The steam temperature at 30 m depth, as predicted by the model, is 25°C above the borehole wall temperature at the same depth. As Figure 3.7 illustrates, steam flowing uphole can cause a significant modification to the formation temperature in the immediate vicinity of the borehole. The net result of these effects is measured borehole temperatures that do not represent true formation temperatures. Since a steam velocity of 0.6 m/s is a reasonable value for 79-5, based on visual observation, the temperature measurements in 79-5 should be regarded with caution. Differences between measured and true formation temperature could be as high as 125°C.

During the month of March, 1980, Kilauea Iki received approximately 2 m of rain. Figure 3.8 illustrates the cooling effect the rain had on the upper 50 m of the 79-5 borehole. The energy required to cool a 1 m^2 by 50 m deep section of the formation to the extent implied by the figure, can be estimated to be

$$\Delta E_f = mC_p \Delta T = (50\ m^3)(2700\ kg/m^3)(1046\ J/kg\text{-}°C)(85°C) \qquad (3.15)$$

$$= 1.20 \times 10^{10}\ J$$

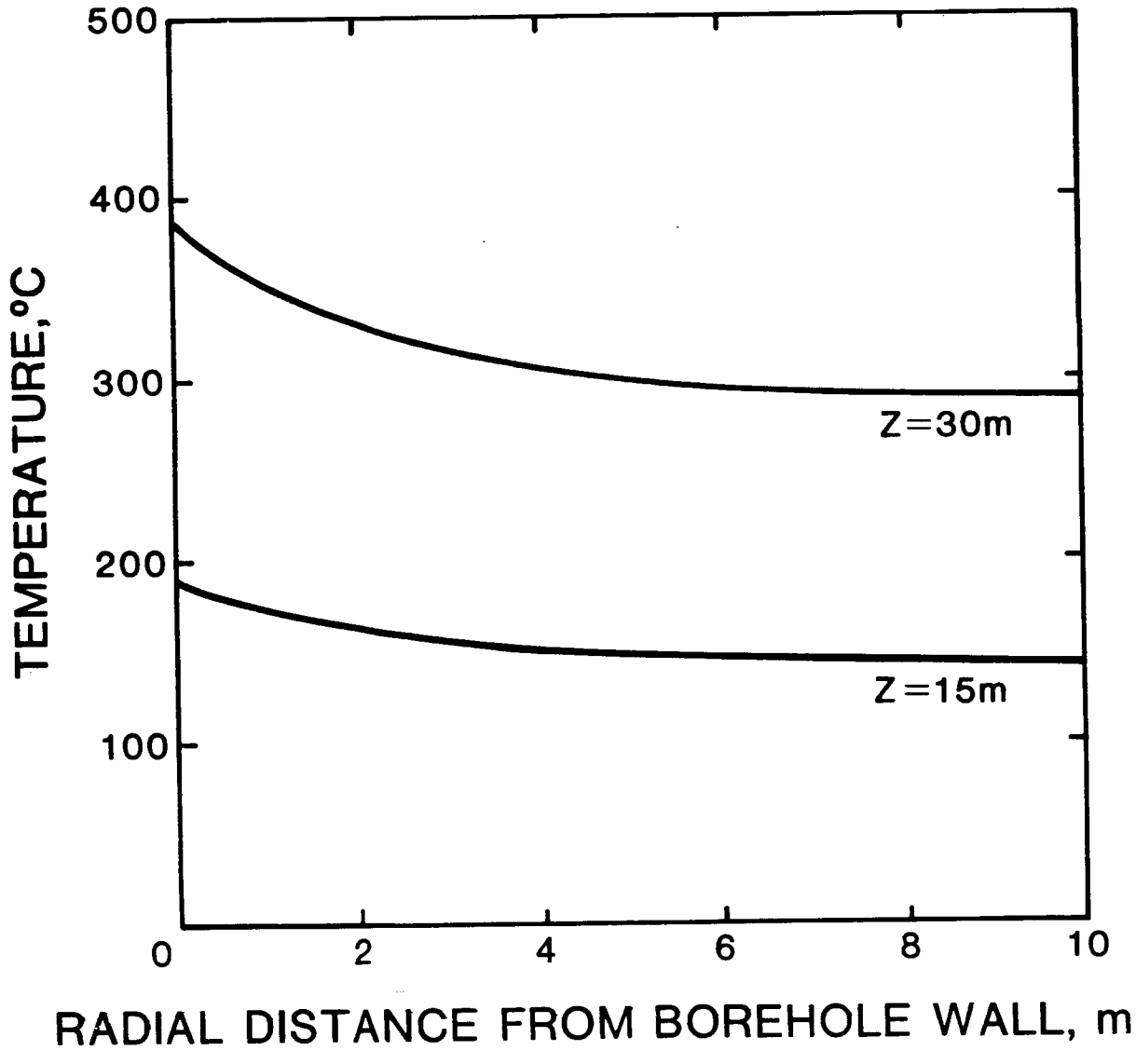

FIGURE 3.7 RADIAL TEMPERATURE DISTRIBUTION

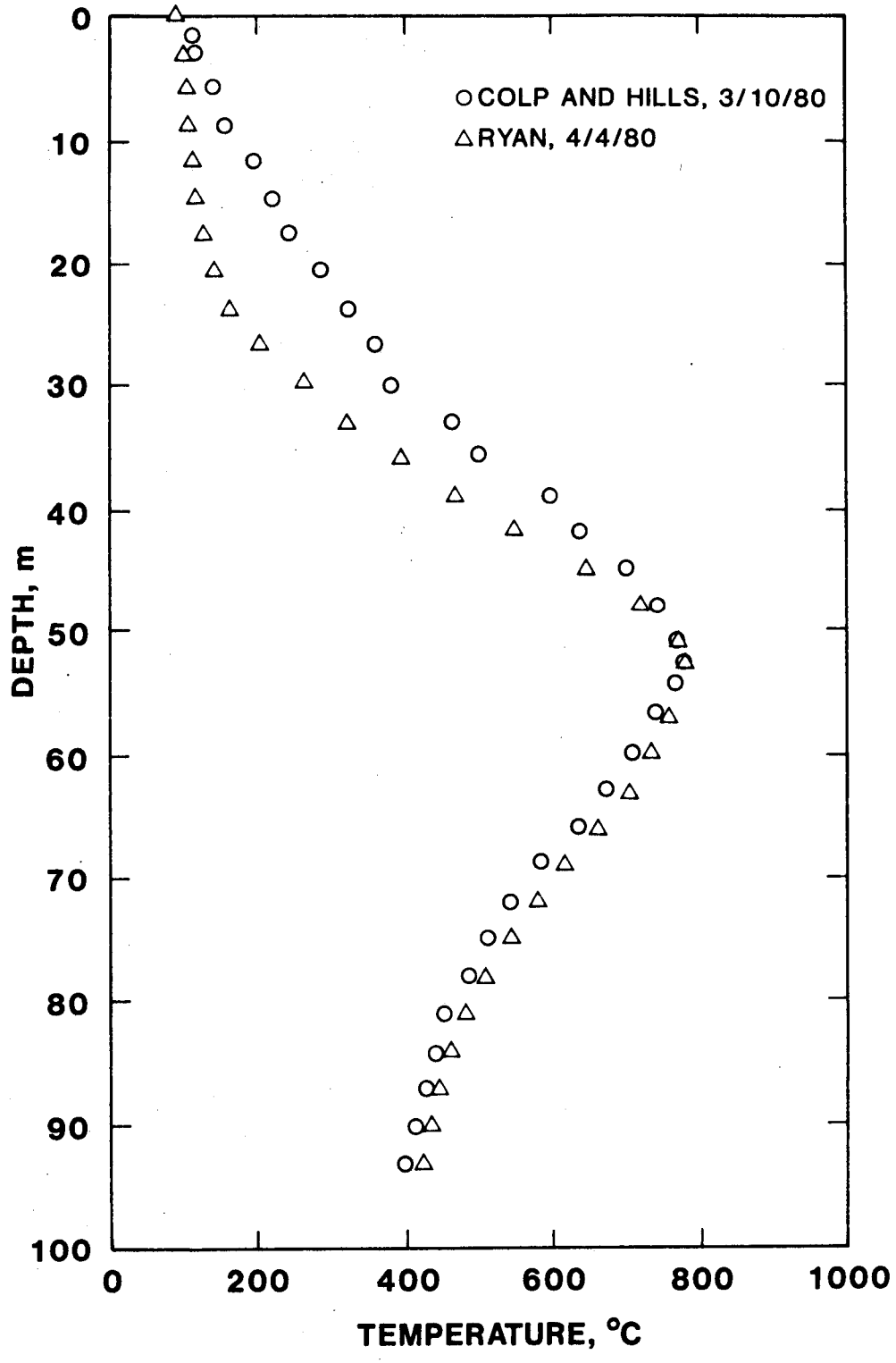

FIGURE 3.8 EFFECT OF RAIN IN 79-5

The amount of energy available for vaporization of 2 m of 20°C rain that falls on 1 m^2 area can be estimated to be

$$\Delta E_r = m\Delta u = (2\ m^3)(1000\ kg/m^3)(2.42 \times 10^6\ J/kg) \qquad (3.16)$$

$$= 4.84 \times 10^9\ J$$

So

$$\frac{\Delta E_f}{\Delta E_r} = 2.5 \qquad (3.17)$$

Therefore, 2.5 times as much rain would have had to fall, assuming 100% vaporization, for the formation to decrease in temperature by the suggested amount. This observation suggests the idea that only the formation near the borehole was cooled by the observed amount. A steam heated borehole would cool at an accelerated rate due to the large horizontal advection of steam into the low pressure borehole from the surrounding formation. Although the observed rain effect does not conclusively prove that the temperatures in the 79-5 borehole are altered by steam, it does lend support to the idea.

The elimination of the steam effect on a borehole requires that the uphole mass flow rate of the steam be reduced. Numerical experiments indicate that an uphole flow rate of 1 cm/s in 79-5 for a year results in an error of only 2°C. To reduce the flow rate of steam, the hole must be cased effectively, and the casing must be sealed at the bottom.

Previous tests (see Colp, 1979) indicate that the steam effect is not significant over the center of the lake. This result is probably due to the impermeable molten lens acting as a barrier to

convection from depth. The steam in the region above 100°C above the magma is essentially stagnant (Hardee, 1980). After the magma body solidifies, however, steam could rise from depth through newly formed thermal fractures. Because of the steam effect, all future temperature holes at Kilauea Iki should be adequately cased or sealed.

4.0 Conclusions

Although the cooling of Kilauea Iki lava lake has been the subject of much study, the only region in which the cooling dynamic models have been well tested is the region above the center of the magma lens. In this region, the lake appears to have passed through two stages. In the first stage, the heat flux from the cooling magma body is sufficient to boil off any meteoric water falling on the lake. The upper solidification front moves downward with the square root of time.

During the second stage, the heat flux from the magma body is not sufficient to boil off all the meteoric water above the body. This results in a two phase zone above a transition zone. In the transition zone, the temperature increase from the boiling point of water to the magma temperature occurs in approximately 10 m. During this stage of heat transfer, heat is removed from the upper surface of the magma body at a constant rate. This rate is controlled by the permeability of the formation. As a result of the constant heat flux, the upper solidification front moves downward at a constant rate.

In the third stage of solidification, the velocity of the solidification fronts increase due to the close proximity of the upper and lower fronts. This stage ends when the two fronts coincide. There is no conclusive evidence that the center of Kilauea Iki is in this stage of

cooling at the present time.

In the remaining stages of cooling, the lake cools to a point where fractures exist throughout (stage 4), which leads to possible hydrothermal convection throughout the lake (stage 5). The lake remains in stage 5 until it cools to a point where no superheated steam exists. At this point the lake enters stage 6 and cools to ambient. Until field verification is possible, the suggested mechanisms of heat transfer for Kilauea Iki during stages 3 through 6 can only be speculative.

While there are presently no temperature measurements in the region below the partial melt, petrological data (Luth, Gerlach and Eichelberger, 1981) suggest that the lower 1070°C isotherm is at approximately 90 m depth. This depth is consistent with that inferred from a simple conduction model for the the solidification of the lava lake from below.

Numerical experiments indicate that the temperatures observed in the margin hole (79-5) are altered by steam flow uphole. Differences between measured and true formation temperatures can be as high as 125°C after only 11 months of steam heating. In order to reduce this problem, the hole must be sealed or cased so as to slow the upflowing steam.

While much is known about the cooling of Kilauea Iki lava lake from above, little information is available that adequately supports cooling models for the regions on the margins or below the solidifying melt. Only direct temperature measurements in conjunction with petrological data can resolve this problem.

REFERENCES

Carslaw, H. S., and Jaeger, J. C. (1959). Conduction of Heat in Solids, Clarendon Press, Oxford, Great Britain, pp 282-296.

Chapman, A. J. (1974), Heat Transfer. Macmillan Publishing Co., Inc., New York, p 344.

Cheng, P. and Minkowycz, W. J. (1977). Free Convection About a Vertical Flat Plate Embedded in a Porous Medium with Application to Heat Transfer from a Dike, J. of Geophysical Research, Vol 82, pp 2040-2044.

Colp, J. L., and Okamura, R. T. (1978). Drilling into Molten Rock at Kilauea Iki, Proceedings of the Geothermal Resource Council, Hilo, Hawaii.

Colp, J. L. (1979). FY79 Lava Lake Drilling Program--Geoscience Studies: Plans and Results, SAND79-1361, Sandia Laboratories, Albuquerque, NM.

Colp, J. L. (1980). Unpublished drilling logs, Sandia Laboratories, Albuquerque, NM.

Colp, J. L., and Striker, R. P. (1980). Personal communication, Sandia Laboratories, NM.

Colp, J. L. (1981). FY80 Annual Progress Report--Magma Energy Research Project, SAND81-0100, Sandia National Laboratories, Albuquerque, NM.

Dunn, J. C., and Hills, R. G. (1980). FY81 Kilauea Iki Lava Lake Experiment Plans, SAND81-1653, Sandia Laboratories, Albuquerque, NM.

Dunn, J. C. (1981). Unpublished drilling logs, Sandia Laboratories, Albuquerque, NM.

Hardee, H. C. (1976). Boundary Layer Solutions for Natural Convection in Porous Media, SAND76-0075, Sandia Laboratories, Albuquerque, NM.

Hardee, H. C. (1980). Solidification in Kilauea Iki Lava Lake, J. of Volcanology and Geothermal Research, Vol. 7, pp 211-233.

Hickox, C. E. (1977). Steady Thermal Convection at Low Rayleigh Number from Concentrated Sources in Porous Media, SAND77-1529, Sandia Laboratories, Albuquerque, NM.

Luth, W. C, Gerlach, T. M., and Eichelberger, J. C. (1981), Major Element Geochemistry of a Magma at Magmatic Conditions, submitted to Science.

Norton, D., and Knight, J. (1977). Transport Phenomena in Hydrothermal Systems: Cooling Plutons, American Journal of Science, Vol. 277, pp 937-981.

Parmentier, E. M. (1979). Two Phase Natural Convection Adjacent to a Vertical Heated Surface in a Permeable Medium, Int. J. of Heat and Mass Transfer, Vol 22, pp 849-855.

Peck, D. L., Moore, J. G., and Kojima, G. (1964). Temperatures in the Crust and Melt of Alae Lava Lake, Hawaii, after the August 1963 Eruption of Kilauea Volcano--a Preliminary Report, U.S. Geological Survey Professional Paper 501-D:6.

Peck, D. L. (1978). Cooling and Vesiculation of Alea Lava Lake, Hawaii, U.S. Geological Survey Professional Paper 935-B.

Richter, D. H., and Moore, J. G. (1966). Petrology of the Kilauea Iki Lava Lake Hawaii, U.S. Geological Survey Professional Paper 537-B.

Ryan, M. L. (1979). High-Temperature Mechanical Properties of Basalt, PhD Pennsylvania State University, Pennsylvania.

Schubert, G., and Straus, J. M. (1979). Steam-Water Counterflow in Porous Media, J. of Geophysical Research, Vol. 84, pp. 1621-1628.

Straus, J. M., and Schubert, G. (1977). Thermal Convection of Water in a Porous Medium: Effects of Temperature and Pressure-dependent Thermodynamics and Transport Properties, J. of Geophysical Research, Vol 82, pp 325-333.

Distribution:

DOE/TIC-4500-R67 UC-66 (235)

Massachusetts Institute of
Technology
Department of Earth Science
Cambridge, MA 02139
Attn: Keiiti Aik, 54-526

Lawrence Berkeley Laboratory (3)
University of California
Berkeley, CA 94720
Attn: J. A. Apps
I. S. Carmichael
P. A. Witherspoon

Shigeo Aramaki
Earthquake Research Institute
University of Tokyo
Bunkyo-ku
Tokyo 113, Japan

U. S. Department of Energy (4)
Division of Geothermal Energy
Washington, DC 20545

United National Institute for
Trn & Res (UNITAR)
801 United Nations Plaza
New York, NY 10017
Attn: J. Barnea, Special Fellow

Sveinbjorn Bjornsson
Science Institute
University of Iceland
Bunhaga 3
107 Reykjavik, Iceland

Argonne National Laboratory
9700 South Cass Avenue
Argonne, IL 60439
Attn: M. Blander, Building 205

Office of Nuclear and Energy
Technology Affairs
Department of State
Washington, DC 20520
Attn: J. L. Bloom

Oregon State University
Corvallis, Oregon 97331
Attn: G. Bodvarsson

University of Texas
Engineering - Science Building
623
Austin, TX 78712
Attn: F. S. Bostick

Stanford University
Petroleum Engineering Department
Stanford, CA 94306
Attn: W. E. Brigham

Los Alamos National Laboratory (6)
P. O. Box 1663
Los Alamos, NM 87545
Attn: R. Brownlee, G-DO, MS 570
C. E. Holley, CNC-2, MS 738
A. W. Laughlin, G-6, MS 978
R. E. Reicker, G-DOT, MS 26
M. C. Smith, G-DOT, MS 26
C. Herrick, CMB-8

State University of New York at
Albany
E215
1400 Washington, Avenue
Albany, NY 12222
Attn: K. Burke

U. S. Geological Survey (6)
345 Middlefield Road
Menlo Park, CA 94025
Attn: R. Christiansen
W. A. Duffield, MS 18
J. G. Moore
H. Shaw, MS 18
P. Ward
H. Iyer

U. S. Geological Survey (2)
Hawaiian Volcano Observatory
Hawaii Volcanoes National Park
Hawaii 96718
Attn: R. W. Decker
Library

University of Texas
Center for Energy Studies
Austin, TX 78712
Attn: M. Dorfman

U. S. Geological Survey (2)
Cascade Volcano Observatory
5400 MacArthur Blvd
Vancouver, WA 98661
Attn: Don Peterson
R. Holcomb

U. S. Geological Survey (5)
956 National Center
Reston, VA 22092
Attn: R. T. Helz, MS 959
D. Peck, Director
R. Tilling, MS 906
C. Zablocki, MS 906
M. Ryan, MS 959

Ingvar B. Fridleifsson
National Energy Authority
Laugavegur 116
Reykjavik, Iceland

Texas A&M University (2)
Dean of Geosciences
College Station, TX 77843
Attn: G. Eaton
M. Friedman

U. S. Geological Survey
Box 25046
Denver Federal Center
Denver, CO 80225
Attn: F. Frischknecht, MS 964

University of Hawaii (2)
Hawaii Institute of Geophysics
Honolulu, Hawaii 96822
Attn: C. Helsley, Head
A. S. Furumoto

Dartmouth College (2)
Hanover, NJ 03755
Attn: R. E. Stoiber
C. Drake

Brown University
Department of Geological Sciences
Providence, RI 02912
Attn: J. F. Hermance

Thomas A. Ladd
Geothermal Program Manager
Department of Energy
200 Stovall Street
Alexandria, VA 22332

University of Alaska
Geophysical Institute
Fairbanks, Alaska 99701
Attn: J. Kielne

U. S. Department of Energy (10)
Office of Basic Energy Science
Washington, DC 20545
Attn: G. A. Kolstad, MS J-309

Oak Ridge National Lab
P. O. Box X
Oak Ridge, TN 37830
Attn: W. L. Marshall

Kazuaki Nakamura
Earthquake Research Institute
University of Tokyo
Hongo
Tokyo 113, Japan

Hans-Ulrich Schmincke
Rohr-Universitat Bochum
Institut fur Mineralogie
D-463 Bachum Postfach 102148
West Germany

Daisuke Shimozuru
Earthquake Research Institute
University of Tokyo
Bunkyo-ku
Tokyo 113, Japan

University of Minnesota
Institute of Technology
107 Lind Hall
207 Church Street, SE
Minneapolis, MN 55455
Attn: Dean Roger Staehle

Superintendent
Hawaii Volcanoes National Park
Hawaii 96718

New Mexico Institute of Mining
and Technology
Department of Geoscience
Socorro, NM 87801
Attn: A. Sanford

Captain William J. Barattino,
P.E., USAF
Chief, At Energy Liaison Office
Department of Energy
Albuquerque Operations Office
P. O. Box 5400
Albuquerque, NM 87185

University of Hawaii
Hawaii Geothermal Project
240 Holmes Hall
2540 Dole Street
Honolulu, Hawaii 96822
Attn: P. C. Yuen

Dr. Richard Tascheck
2035 47th Street
Los Alamos, NM 87544

University of Texas at Dallas
P. O. Box 688
Institute of Geosciences
Richardson, TX 75080
Attn: R. Ward

Conoco, Inc. (3)
P. O. Box 1267
Ponca City, OK 74601
Attn: A. L. Thomas
B. K. Sternberg
S. K. Sahai

Chevron Resources Company
P. O. Box 4001
Golden, CO 80401
Attn: C. M. Swift, Jr.

University of Oregon (2)
Eugene, Oregon 97403
Attn: A. McBirney
H. Waff

Geophysical Laboratory of
Carnegie Institution
2801 Upton Street, NW
Washington, DC 20008
Attn: H. Yoder

Colorado School of Mines
Golden, CO 80401
Attn: J. Applegate

Southern Methodist University
217 N. L. Heroy Hall
Dallas, TX 75275
Attn: David D. Blackwell

Phillips Research Center
Bartlesville, OK 74004
Attn: G. Hoover

Sunoco Geothermal
12700 Mark Central Place
Suite 1500
Dallas, TX 75251
Attn: A. Ramo

Shell Research
P. O. Box 481
Houston, TX 70001
Attn: R. Thayer

Union Oil Geothermal
2099 Range Avenue
Santa Rosa, CA 95406
Attn: R. Dondanville

Cornell University
Department of Geological Sciences
Ithaca, NY 14853
Attn: S. Kaufman

Systems, Science and Software
P. O. Box 1620
La Jolla, CA 92038
Attn: P. Goupillaud

Technical Consultant
Subcommittee on Adv Energy and
Technologies
House Committee on Science
and Technology
Rayburn Office Building B374
Washington, DC 20515

New Mexico State University (10)
Department of Mechanical Engr
Box 3450
Las Cruces, NM 88003
Attn: R. G. Hills

4000 A. Narath
4700 J. H. Scott
4740 R. K. Traeger
4743 H. C. Hardee (5)
4743 J. L. Colp
4743 J. C. Dunn
4743 L. K. Riddle
4743 R. K. Striker
4750 V. L. Dugan
5000 J. K. Galt
5500 O. E. Jones
5510 D. B. Hayes
5512 D. McVey
5541 W. C. Luth
5541 T. M. Gerlach
5800 R. S. Claasen
5820 R. E. Whan
5822 E. J. Graeber
5830 M. J. Davis
5836 J. L. Ledman
8214 M. A. Pound
3141 L. J. Erickson (5)
3151 W. L. Garner (3)